 doi:10.20944/preprints201904.0299.v1

Green synthesis, structural, in vitro and vivo bioactivity properties of ZnO nanoparticles for biomedical applications

Essam H. Ibrahim[1,2], Obaid Albulym[1], Omer Kaygili[3], Mona Kilany[4,5], Mohd. Shkir*[6], Mai S.A. Hussien[7,8], Niyazi Bulut[3], I.S. Yahia[6,8]

[1]Biology Department, Faculty of Science, King Khalid University, P.O. Box 9004, Abha 61413, Saudi Arabia
[2]Blood Products Quality Control and Research Department, National Organization for Research and Control of Biologicals, Cairo, Egypt.
[3]Department of Physics, Faculty of Science, Firat University, 23119 Elazig, Turkey
[4] Biology Department, Faculty of Sciences and Arts, King Khalid University, Dhahran Al Janoub, Saudi Arabia.
[5]Department of Microbiology, National Organization for Drug Control and Research (NODCAR), Cairo, Egypt
[6]Advanced Functional Materials & Optoelectronic Laboratory (AFMOL), Department of Physics, Faculty of Science, King Khalid University, P.O. Box 9004, Abha, Saudi Arabia.
[7]Department of Chemistry, Faculty of Education, Ain Shams University, Roxy, 11757 Cairo, Egypt
[8]Nanoscience Laboratory for Environmental and Bio-medical Applications (NLEBA), Semiconductor Lab., Metallurgical Lab.1. Department of Physics, Faculty of Education, Ain Shams University, Roxy, 11757 Cairo, Egypt.

***Corresponding author**
Dr. Mohd. Shkir
Assistant Professor
Department of Physics, KKU, Abha, KSA
E-mail: shkirphysics@gmail.com

 doi:10.20944/preprints201904.0299.v1

Abstract

Owing to fascinating applications of ZnO in modern devices, it is interesting to explore its more features for future devices. Hence, herein, we have synthesized the high quality ZnO spherical nanoparticles (SNPs) through a facile green synthesis route and robust structural and biomedical studies are carried out. Hexagonal phase with 93.2% crystallinity was confirmed through XRD analysis. ZnO nanoparticles were tested for their bioactivities both *in vivo* (acute cytotoxicity test) and *in vitro* (Anti-cancer activities on liver (HepG2) and cervical (Hela) cancer cell lines, stimulatory/inhibitory effects on normal rat splenic cells and hemolytic effects on red blood cells). Results showed that ZnO SNPs has no cytotoxic effects on vital organ like liver and has no hemolytic action on red blood cells. ZnO SNPs showed inhibitory consequence on normal rat splenic cells growth at all tested concentrations. ZnO nanoparticles showed an inhibitory effect on HepG2 cell line. While showed stimulatory effect on Hela cell line. Current study presents the synthesized ZnO SNPs as highly applicable in bio-optoelectronics.

Keywords: X-ray diffraction; bioactivities; cytotoxicity test; Anti-cancer activities

1. Introduction

Zinc oxide (ZnO) is an excellent semiconductor which possess high chemical stability, biocompatibility, bio-safe, non-toxicity, environmental friendly and low cost material, and have vast applications [1-3]. ZnO has a direct wide-energy gap of 3.37 eV and an excitation strap energy of 60 meV at RT [4,5]. ZnO has been widely used in the radiation dosimeters, radiation detectors [6], light emitting diodes [7], transistors [8], solar cells [9], biomedical applications [10], catalysts [11], energy storage devices [12], memristors [13], photodetectors [14] and gas sensors [15]. The improvement in antibacterial effect of ZnO coating on the gutta-percha cone was reported by Alves *et al.* [16]. The antimicrobial activity of ZnO against Staphylococcus

Preprints (www.preprints.org) | NOT PEER-REVIEWED | Posted: 26 April 2019 doi:10.20944/preprints201904.0299.v1

aureus, *Escherichia coli* and *Candida albicans* was reported by Raafat *et al.* [17]. Rajiv *et al.* [18] studied on the phytotoxicity of *Eichhornia crassipes* assisted ZnO samples sprayed on *Helianthus annuus* and reported that high amounts of ZnO cause the phytotoxicity. Pathak *et al.* [19] synthesized the pure, Ag-doped and Au-doped ZnO samples, studied their antibacterial activities against *E. coli*, *S. aureus* and *E. ashbyii* and showed that the pure ZnO was more effectual against *E. coli* and *S. aureus* in comparison to the doped samples. After testing the antimicrobial activity of ZnO against *A. baumannii* and *P. aeruginosa* cultures, Khatami *et al.* [20] reported that it can be used for producing the clinical antimicrobial wound-healing bandages in order to treat and wrap the infection receptive wounds like: burns and diabetic wounds. The pure, polyethylene glycol- and polyvinyl pyrrolidone-assisted ZnO samples were synthesized by Javed *et al.* [21], and they reported that these additives improve the antibacterial activity of ZnO.

In the present paper, we prepared high quality spherical ZnO nanoparticles through a sample flash combustion method and determined its structural, morphological and *in vivo* and *in vitro* bioactivities and discussed.

2. Material and Methods

2.1. Synthesis and characterization

For bio/green synthesis of ZnO, we have weighed ~ 10 g of Zinc nitrate hexahydrate ($Zn(NO_3)_2 \cdot 6H_2O$), procured from Sigma-Aldrich and 1g of citric acid was added to it in a ceramic crucible of 100 ml capacity. Proper mixing was carried out through a mortar and kept inside the highly stable furnace at 450 °C for about 2 hours. After the mentioned time the furnace was switched off to be naturally cooled down to RT. Finally, the white material was taken from crucible and studied.

X-ray diffraction (XRD) spectrum of the as-produced ZnO in the 2θ range of 10-80° was collected using a Shimadzu XRD-6000 diffractometer, operated at 30 kV and 30mA, using CuK_α

Preprints (www.preprints.org) | NOT PEER-REVIEWED | Posted: 26 April 2019 doi:10.20944/preprints201904.0299.v1

radiation with the wavelength of 0.1543 nm. The morphology was investigated using a JEOL 7500F field emission scanning electron microscope (FESEM) operated at 20 kV.

2.2. Antimicrobial susceptibility testing (AST)

2.2.1. Test Microorganisms

The antimicrobial action of ZnO nanoparticles was assessed against E coli, Pseudomonas aeruginosa (Gram negative), Staphylococcus aureus, Bacillus subtilis (Gram positive), and Candida albicans (as a model of yeast) compared to tetracycline (30 µg) as a positive control. Overnight cultures were kept for 24 h at 36ºC ± 1ºC and bacterial deferment (inoculum) was thinned with sterile saline solution to 108 CFU/ml (McFarland standard: OD= 0.5 at 600 nm).

2.2.2. Agar disk diffusion method

Agar-disk-diffusion methodology was adopted according to Shkir *et al.* [22] to assess the antimicrobial activity of ZnO NPs using Muller Hinton agar media. The experiment was conducted in triplicate.

2.3. *In vitro* effects of ZnO nanoparticles on splenic cells proliferation

2.3.1. Splenic cells culture preparation

The test was done as per Ibrahim *et al.* [23] with slight changes. Spleen of a healthy adult male Sprague Dawley rat weighing about 0.280 kg, kindly provided by animal house at King Khalid University, and used to obtain splenic cells. The rat was killed by cervical dislocation and spleen was aseptically removed and transferred into Petri dishes (100 X 15 mm, Falcon) containing serum-free complete RPMI-1640 medium (SFM) (consisting of RPMI-1640 medium (Gibco), supplemented with penicillin/streptomycin 100 U/100 µg/ml (Gibco), 2 mM L-glutamine (Gibco), 2 mM sodium pyruvate (Seromed), 2% sodium bicarbonate (Seromed), pH 7.2 and HEPES (*N*-2-hydroxyethylpiperazine-*N*-2-ehtanesulfonic acid) buffer (Sigma)). The spleen was minced into

Preprints (www.preprints.org) | NOT PEER-REVIEWED | Posted: 26 April 2019 doi:10.20944/preprints201904.0299.v1

single cell suspension and passed through 70 µm mesh (Spectrum) into 15 mL centrifuge tube (Falcon) to remove clumps. The deferral was centrifuged at 1,000 rpm for 8 min and 1 mL ACK lysis buffer (Gibco) was added to the re-suspended cell pellet for 3 min at room temperature to rupture red blood corpuscles. The lytic action of ACK buffer was reduced by adding SFM. Cell viability was monitored by trypan blue dye exclusion test [24]. Cells were adjusted to $0.06X10^6$/mL in SFM supplemented with 10% fetal calf serum (Gibco) (culture medium). The activity of cell culture was carried out in micro-well tissue culture plate (Techno Plastic Products, Trasadingen, Switzerland).

2.3.2. Study of cytotoxic/proliferative effects ZnO nanoparticles

Cytotoxic (cell's killing) or proliferative (induction of normal cell's proliferation) prospective which might be available in ZnO nanoparticles were tested by adding 100 µL dissimilar concentrations of ZnO nanoparticles such as: 6, 12.5, 25, 50 and 100 µg/mL to wells containing 100 µL of cell suspension (6000 cells/well) separately in triplicates. Cells without ZnO nanoparticles were included as normal cell-control. Saucers containing the cells were incubated at 37 °C for 72 hours in 5% CO_2 (Memmert, Gmbh) [25]. Vybrant® MTT Cell Proliferation Assay Kit (Thermo Fisher Scientific) was used as per instructions to calorimetrically compute the change in cell numbers of diverse treated cells [23]. The outputs were articulated as a % of enlarge/reduce in growth, as per Oves *et al.* [26].

2.4. Lytic effects of ZnO nanoparticles suspension on red blood cells

The lytic effects of ZnO nanoparticles were determined by using the method described by Oves *et al.* [26] with some modifications. ZnO nanoparticles at a concentration of 1 mg/mL in sterile phosphate buffered saline (PBS, pH 7.4) was prepared. Thirty mL of freshly obtained cow blood was positioned in 50-mL Falcone tube having EDTA to avoid coagulation, gently grind and then separated into numerous sterile 15 mL Falcon tubes and centrifuged for 5 min at 1000 ×

Preprints (www.preprints.org) | NOT PEER-REVIEWED | Posted: 26 April 2019 doi:10.20944/preprints201904.0299.v1

g. The supernatant was poured off and RBCs were washed three times with chilled (4 °C) PBS. The washed RBCs were re-suspended in chilled PBS to get 10 % hematocrit. A 100 µL of prepared ZnO SNPs were added to 900 µL of prepared RBCs in 1.6 mL Eppendorf tubes and incubated for 60 min at 37 °C. 1% Triton X-100 was taken as a positive control and PBS as a negative control. All the tubes were subjected to centrifuge for ~ 10 min at 2000 RPM and then absorbance were measured at 576 nm (Lamda 25- Perkin Elmer).

2.5. Acute cytotoxicity study of ZnO nanoparticles

To test hepatic toxicity which may be found ZnO nanoparticles, 5 adult healthy rats (200-250 g) were injected with a mono dose regimen of 100 µg/mL ZnO nanoparticles [26]. The rats were left for 24 h and then sacrificed and sera were obtained from their blood. Liver function was tested by assaying the levels of serum aspartate aminotransferase (AST) and alanine aminotransferase (ALT) colorimetrically according to the Reitman and Frankel method using Randox Kit (UK).

2.6. Effects of ZnO nanoparticles on Hela and HepG2 cancer cell lines

HepG2 and HeLa cell lines (Sigma-Aldrich) were cultured separately in DMEM (Sigma) supplemented with 10% fetal calf serum (Gibco BRL), penicillin/streptomycin (100 U/ml/100 mg/ml, Gibco BRL) and 2 mM L-glutamine (Gibco BRL) at cell density of 5000 cells/well in 96-well tissue culture plate (Falcon). Plates were incubated at 37 °C under 5% CO_2 and 90% humidity for 24 h. The media was removed from each plate and replaced with 200 µL/well fresh media containing 100 or 50 µg/mL ZnO nanoparticles separately. Cells with media only served as control culture. The cultures were continued for more 24 h at the same conditions described above. Cell viability assay was done according to Ibrahim et al. [23] using Vybrant® MTT Cell Proliferation Assay Kit (Thermo Fisher Scientific) with little modifications. The media in microwell plates were changed with 100 µL fresh culture medium and 10 µL of 12 mM MTT

Preprints (www.preprints.org) | NOT PEER-REVIEWED | Posted: 26 April 2019 doi:10.20944/preprints201904.0299.v1

were add to each well and left for 3 h. Then, to each well 100 µL of 0.1% acidified sodium dodecyl sulphate (SDS) were added to each well and the absorbance was read at 570 nm.

The outputs are presented ar % of manage at end of every incubation stage [27].

3. Results and discussion

3.1. XRD analysis

The XRD pattern of as-synthesized ZnO is shown in Fig. 1a. This pattern is matched with the reported one for the wurtzite structure of ZnO having the hexagonal crystal structure (JCPDS PDF No: 79-0205) [28, 29]. The as-observed peaks of the planes of (100), (002), (101), (102), (110), (103), (200), (112), (201), (004) and (202) indicate the polycrystalline structure of the as-produced ZnO sample. There is no impurity phase detected, that is, the purity of the as-synthesized ZnO is 100%.

The crystallinity percent (X_C%) was computed according to Ref. [30], and this value was calculated to be 93.2%, indicating the high crystallinity.

The lattice constants (a and c) and cell volume (V) of ZnO sample were estimated from Eqs. (1) and (2), respectively [31]:

$$\frac{1}{d^2} = \frac{4}{3}\left(\frac{h^2 + hk + k^2}{a^2}\right) + \frac{l^2}{c^2}, \quad \textbf{(1)}$$

$$V = 0.866 a^2 c, \quad \textbf{(2)}$$

where d is the distance for two adjacent plane and h, k and l are known as the Miller indices. The as-calculated values are a=0.324268 nm, c=0.519762 and V=0.047329 nm^3.

The crystallite size (D_S) was attained from following Scherrer's and Williamson-Hall (D_{WH}) rules, correspondingly [32]

$$D_S = \frac{0.9\lambda}{\beta \cos\theta}, \quad \textbf{(3)}$$

Preprints (www.preprints.org) | NOT PEER-REVIEWED | Posted: 26 April 2019 doi:10.20944/preprints201904.0299.v1

$$\beta \cos\theta = \frac{0.9\lambda}{D_{WH}} + 4\varepsilon \sin\theta, \quad \textbf{(4)}$$

where β is FWHM, θ is Bragg angle, λ is wavelength, which equals to 0.1543 nm for Cu Kα radiation and ε is lattice strain. The D_{WH} and ε were calculated from the $\beta\cos\theta$ vs. $4\sin\theta$ plot shown in Fig. 1b. The ε value was found to be 0.476×10^{-3}. The D_S and D_{WH} were estimated to be 21.17 and 23.58 nm, respectively.

The Young's modulus (Y) value for each Miller indices was calculated by [32]

$$Y = \frac{\left[h^2 + \frac{(h+2k)^2}{3} + \left(\frac{al}{c}\right)^2\right]^2}{s_{11}\left(h^2 + \frac{(h+2k)^2}{3}\right)^2 + s_{33}\left(\frac{al}{c}\right)^4 + (2s_{13} + s_{44})\left(h^2 + \frac{(h+2k)^2}{3}\right)\left(\frac{al}{c}\right)^2}, \quad \textbf{(5)}$$

where the elastic compliances of s_{11}, s_{13}, s_{33} and s_{44} have been reported in the literature to be 7.858×10^{-12}, -2.206×10^{-12}, 6.940×10^{-12} and 23.570×10^{-12} $m^2.N^{-1}$, respectively.

Using the Y values for each Miller indices observed on the XRD pattern of the as-produced ZnO, the stress (σ) in the surface and energy density (u) were estimated by [32]:

$$\beta \cos\theta = \frac{0.9\lambda}{D_{WH}} + \frac{4\sigma \sin\theta}{Y}, \quad \textbf{(6)}$$

$$\beta \cos\theta = \frac{0.9\lambda}{D_{WH}} + 4\sin\theta\left(\frac{2u}{Y}\right)^{1/2}, \quad \textbf{(7)}$$

The σ and u values were estimated from the $\beta\cos\theta$ vs. $4\sin\theta Y^{-1}$ and $\beta_{hkl}\cos\theta_{hkl}$ vs. $2^{5/2}\sin\theta_{hkl}\,Y_{hkl}^{-1/2}$ plots shown in Figs. (1c&1d), and found to be 37.227 MPa and 9.707 kJ m^{-3}, respectively. These results are in well accord to prevous results (28 MPa and 8.65 $kJ.m^{-3}$) given in the literature for ZnO sample prepared using methanol by Thandavan *et al* [33]. The following relation was used to calculated the bond length (L) between Zn and O [32]:

Preprints (www.preprints.org) | NOT PEER-REVIEWED | Posted: 26 April 2019 doi:10.20944/preprints201904.0299.v1

$$L = \sqrt{\frac{a^2}{3} + c^2\left(0.25 - \frac{a^2}{3c^2}\right)^2}\,, \qquad \textbf{(8)}$$

The L value was computed to be 0.197375 nm, and this is very close to the reported one (0.19767 nm) [34]. Atomic packing factor (*APF%*) was computed from the following relation [35]:

$$APF\,\% = \frac{2\pi a}{3\sqrt{3}c} \times 100\,, \qquad \textbf{(9)}$$

The *APF%* of the sample was found to be 75.401 %. This is so close to the reported result for the pure ZnO (75.302 %) by Birajdar *et al* [36].

3.2. SEM observations

SEM micrographs captured at magnifications of ×25,000 and 40,000× are exposed in Fig. 2. It is obvious from figure that the prepared ZnO is composed of the stacked-spherical nanoparticles (SNPs) with the particle size distribution ranging from 90 nm to 147 nm.

3.3. Antimicrobial potential

Our findings reported that ZnO nanoparticles exhibited a considerable antimicrobial potential against E coli, *Pseudomonas aeruginosa* (Gram negative), *Staphylococcus aureus, Bacillus subtilis* (Gram positive), and *Candida albicans* (yeast) compared to tetracycline (30 µg) as a positive control as shown in Fig. 3 and Table 1.

Many mechanisms described the antimicrobial activity od ZnO-NPs. The straight contact of ZnO-NPs with bacterial cell walls may results in the devastation of bacterial cell integrity [37-39]. The other expected mechanism is the liberation of antimicrobial ions mainly Zn^{2+} ions [40,41] and the formation of reactive oxygen species (ROS) [42-45].

Preprints (www.preprints.org) | NOT PEER-REVIEWED | Posted: 26 April 2019 doi:10.20944/preprints201904.0299.v1

Though, the mechanism of toxicity differ in a range of medium as the species of liquefy Zn might alter as per the medium components besides the physico-chemical chattels of ZnO-NPs [41].

3.4. Effects on rat splenic cells proliferation

The cytotoxic or stimulatory properties that may be found in the ZnO nanoparticles were studied at different concentrations. The results showed that there were cytotoxic/inhibitory effects of ZnO nanoparticles on normal splenic cells at all tested concentrations (Fig. 4, 5 & Table 2).

ZnO is known to be slightly soluble and capable of releasing Zn^{2+} in solution. It is believed that dissolved Zn^{2+} played an important role in the toxicity of ZnO-NPs [46] and some researchers inferred that toxic effects of ZnO-NPs on cultured cells may be due to the dissolution of Zn^{2+} [47]. Deng et al.11 found that ZnO-NPs and zinc chloride ($ZnCl_2$) had alike toxic consequence on mouse. Moreover, no content of dissolved Zn^{2+} was determined.

Many works have demonstrated the selectivity and toxicity of ZnO-NPs against cancer cells [48-49] indicating its usefulness in cancer fight. However, the therapeutic use of ZnO-NPs may change host immune defences which may have beneficial or deleterious effects. The good side may be represented in that ZnO-NPs increase metallothionein (protein involved in phagocytosis) [50], macrophages antigen presentation [51], and inflammatory responses [52]. In contrary, ZnO-NPs also comprise the prospective to decrease the viability of some immune cells like macrophages [53].

3.5. Lytic effects of ZnO nanoparticles suspension on red blood cells

The cytotoxicity was premeditated by exploratory haemolytic activity alongside cow red blood cells (RBCs) using Triton X-100 as constructive control. The % lysis estimated through comparing the sample absorbance and Triton X-100. The +ve manage demonstrate about 100%

Preprints (www.preprints.org) | NOT PEER-REVIEWED | Posted: 26 April 2019 doi:10.20944/preprints201904.0299.v1

lysis, while the phosphate buffer saline (PBS) displayed no lysis effects on RBCs. The as-prepared ZnO nanoparticles showed no lytic effect on RBCs (Fig. 6(a).

Many workers tested the effects of ZnO-NPs on RBCs but most of them reported the absence of hemolytic effects of ZnO-NPs on RBCs [54-56].

3.6. Acute cytotoxicity study of ZnO nanoparticles

To test hepatic and renal toxicities which may be found in ZnO nanoparticles, adult healthy rats (200-250 g) were injected with a single dose regimen of 100 µg/ml ZnO nanoparticles. After the rats were left for 24 h, their sera were separated from the blood. The serum aspartate aminotransferase (AST) levels and alanine aminotransferase (ALT) showed non-significant increase (1.33 and 1.10 folds respectively) than that of normal group.

We have used an acceptable ZnO-NPs for injection, bur other workers showed hepatocytotoxicity after injecting high dose (50 mg/kg) in rat [57].

3.7. Effects of ZnO nanoparticles on Hela HepG2 cancer cell lines

ZnO nanoparticles showed an inhibitory effect on HepG2 cell line. This effect decreased with the decrease in ZnO nanoparticles concentration (Fig. 6(a)). In contrary, ZnO nanoparticles showed stimulatory effect on Hela cell line. This stimulatory effect was dose dependent as it decreased with the decrease in ZnO nanoparticles concentration (Fig. 6(b)). The mechanisms that cause the toxicity of ZnO may comprise the participation of the generation of ROS and as well as induction of apoptosis [49]. From the all the above cytotoxicity studies we can say that the associated cytotoxicity may be choosy for those cells that construct larger levels of ROS show rapid separating such as immune cells [48], cancer cells [49] and bacteria [58].

4. Conclusions

High quality spherical nanoparticles (SNPs) of ZnO has been synthesized by a simple flash combustion route and explore its possible applications in biomedical field. XRD approved

its single phase of high degree of crystallinity (i.e. 93.2 %). The average value crystallite size was found ~ 21.17 and 23.58 nm obtained through Scherrer's and Williamson-Hall equations. Further several other parameters have been determined through XRD data. Moreover, SEM study reveal the grains size in range from 90 nm to 147 nm. The key studies on ZnO SNPs was done as bioactivities both *in vivo* (acute cytotoxicity test) and *in vitro* (Anti-cancer activities on liver (HepG2) and cervical (Hela) cancer cell lines, stimulatory/inhibitory effects on normal rat splenic cells and hemolytic effects on red blood cells). These typical studies revealed that ZnO SNPs has no cytotoxic effects on vital organ like liver and has no hemolytic action on red blood cells. ZnO SNPs showed inhibitory consequences on normal rat splenic cells growth at all tested concentrations. ZnO SNPs showed an inhibitory effect on HepG2 cell line. While showed stimulatory effect on Hela cell line. On the basis of obtained results it is found that ZnO SNPs are highly applicable in biological applications.

Acknowledgment

The authors express their appreciation to the Deanship of Scientific Research at King Khalid University for funding this work through research groups program under grant number R.G.P.1/17/38.

References

[1] I.N. Reddy, C.V. Reddy, A. Sreedhar, J. Shim, M. Cho, K. Yoo, D. Kim, Structural, optical, and bifunctional applications: Supercapacitor and photoelectrochemical water splitting of Ni-doped ZnO nanostructures, J. Electroanal. Chem. 828 (2018) 124-136.

[2] Z. Li, R. Yang, M. Yu, F. Bai, C. Li, Z.L. Wang, Cellular level biocompatibility and biosafety of ZnO nanowires, J. Phys. Chem. C 112 (2008) 20114-20117.

[3] L. Liu, Z. Liu, Y. Yang, M. Geng, Y. Zou, M.B. Shahza, Y. Dai, Y. Qi, Photocatalytic properties of Fe-doped ZnO electrospun nanofibers, Ceram. Int. 44 (2018) 19998-20005.

[4] L. Fu, Z. Fu, Plectranthus amboinicus leaf extract–assisted biosynthesis of ZnO nanoparticless and their photocatalytic activity, Ceram. Int. 41 (2015) 2492-2496.

[5] X.F. Jia, Q.Y. Hou, Z.C. Xu, L.F. Qu, Effect of Ce doping on the magnetic and optical properties of ZnO by the first principle, J. Magn. Magn. Mater. 465 (2018) 128-135.

[6] H.A. Thabit, N.A. Kabir, The study of X-ray effect on structural, morphology and optical properties of ZnO nanopowder, Nucl. Instrum. Methods Phys. Res., Sect. A 436 (2018) 278-284.

[7] M.Sathya, K. Pushpanathan, Synthesis and optical properties of Pb doped ZnO nanoparticless, Appl. Surf. Sci. 449 (2018) 346-357.

[8] J.H. Park, P. Biswas, D.K. Kwon, S.W. Han, H.K. Baik, J.M. Myoung, Adopting novel strategies in achieving high-performance single-layer network structured ZnO nanorods thin film transistors, ACS Appl. Mater. Interfaces 8 (2016) 11564-11574.

[9] J.A. Anta, E. Guillen, R. Tena-Zaera, ZnO-based dye-sensitized solar cells, J. Phys. Chem. C 116 (2012) 11413-11425.

[10] H. Mirzaei, M. Darroudi, Zinc oxide nanoparticless: Biological synthesis and biomedical applications, Ceram. Int. 43 (2017) 907-914.

[11] I. Francesco, M. Casiello, A. Monopoli, P. Cotugno, M.C. Sportelli, R.A. Picca, N. Cioffi, M.M. Dell'Anna, A. Nacci, Ionic liquids/ZnO nanoparticless as recyclable catalyst for polycarbonate depolymerisation, J. Mol. Catal. Chem. 426 (2017) 107-116.

[12] K.S. Lee, C.W. Park, S.J. Lee, J.D. Kim, Hierarchical zinc oxide/graphene oxide composites for energy storage devices, J. Alloys Compd. 739 (2018) 522-528.

[13] Y.P. Santos, E. Valença, R. Machado, M.A. Macêdo, A novel structure ZnO-Fe-ZnO thin film memristor, Mater. Sci. Semicond. Process. 86 (2018) 43-48.

[14] S. Noothongkaew, O. Thumthan, K.S. An, UV-Photodetectors based on CuO/ZnO nanocomposites, Mater. Lett. 233 (2018) 313-323.

[15] K.S. Choi, S.P. Chang, Effect of structure morphologies on hydrogen gas sensing by ZnO nanotubes, Mater. Lett. 230 (2018) 48-52.

[16] M.J. Alves, L. Grenho, C. Lopes, J. Borges, F. Vaz, I.P. Vaz, M.H. Fernandes, Antibacterial effect and biocompatibility of a novel nanostructured ZnO-coated gutta-percha cone for improved endodontic treatment, Mater. Sci. Eng. C 92 (2018) 840-848.

[17] A. I. Raafat, N.M. El-Sawy, N.A. Badawy, E.A. Mousa, A.M. Mohamed, Radiation fabrication of Xanthan-based wound dressing hydrogels embedded ZnO nanoparticless: In vitro evaluation, Int. J. Biol. Macromol. 118 (2018) 1892-1902.

[18] P. Rajiv, P. Vanathi, A. Thangamani, An investigation of phytotoxicity using *Eichhornia* mediated zinc oxide nanoparticless on *Helianthus annuus*, Biocatal. Agric Biotechnol. 16 (2018) 419-424.

[19] T.K. Pathak, R.E. Kroon, H.C. Swart, Photocatalytic and biological applications of Ag and Au doped ZnO nanomaterial synthesized by combustion, Vacuum 157 (2018) 508-513.

[20] M. Khatami, R.S. Varma, N. Zafarnia, H. Yaghoobi, M. Sarani, V.G. Kumar, Applications of green synthesized Ag, ZnO and Ag/ZnO nanoparticless for making clinical antimicrobial wound-healing bandages, Sustainable Chem. Pharm. 10 (2018) 9-15.

[21] J.R. Javed, M. Usman, S. Tabassum, M. Zia, Effect of capping agents: Structural, optical and biological properties of ZnO nanoparticless, Appl. Surf. Sci. 386 (2016) 319-326.

[22] M. Shkir, M. Kilany, I.S. Yahia, Facile microwave-assisted synthesis of tungsten-doped hydroxyapatite nanorods: A systematic structural, morphological, dielectric, radiation and microbial activity studies, Ceram. Int. 43 (2017) 14923-14931.

[23] E.H. Ibrahim, M. Kilany, H.A. Ghramh, K.A. Khan, S. Islam, Cellular proliferation/cytotoxicity and antimicrobial potentials of green synthesized silver nanoparticless (AgNPs) using *Juniperus procera*, Saudi J. Biol. Sci. (2018), https://doi.org/10.1016/j.sjbs.2018.08.014.

[24] A. Böyum, Isolation of leucocytes from human blood. A two-phase system for removal of red cells with methylcellulose as erythrocyte-aggregating agent, Scand. J. Clin. Lab. Invest. Suppl. 97 (1968) 9-29.

[25] S. Yashi, K. Yoshiie, H. Oda, M. Sugano, K. Imaizumi, Dietary Curcumaxanthorrhiza Roxb. increases mitogenic responses of splenic lymphocytes in rats, and alters populations of the lymphocytes in mice, J. Nutr. Sci. Vitaminol. 39 (1993) 345–354.

[26] M. Oves, M.S. Khan, A. Zaidi, A.S. Ahmed, F. Ahmed, E. Ahmad, A. Sherwani, M. Owais, A. Azam, Antibacterial and cytotoxic efficacy of extracellular silver nanoparticless biofabricated from chromium reducing novel OS4 strain of Stenotrophomonas maltophilia. PLoS ONE 8 (2013) e59140.

[27] X. Long, R. Matsumoto, P. Yang, T. Uemura, Effect of Human Mesenchymal Stem Cells on the Growth of HepG2 and Hela Cells, Cell Struct. Funct. 38 (2013) 109-121.

[28] J. Ungula, B.F. Dejene, H.C. Swart, Band gap engineering, enhanced morphology and photoluminescence of un-doped, Ga and/or Al-doped ZnO nanoparticless by reflux precipitation method, J. Lumin. 195 (2018) 54-60.

[29] H. Duan, G. Chen, P. Gao, W. Jin, X. Ma, Y. Yin, L. Guo, H. Ye, Y. Zhu, J. Yu, Y. Wu, Crystallography facet tailoring of carbon doped ZnO nanorods via selective etching, Appl. Surf. Sci. 406 (2017) 186-191.

[30] O. Kaygili, Synthesis and characterization of Na_2O–CaO–SiO_2 glass–ceramic, Journal of Thermal Analysis and Calorimetry 117 (2014) 223-227.

[31] B.D. Cullity, Elements of X-ray Diffraction (2nd edition), Addison–Wesley Publishing Company, Massachusetts (1978).

[32] O. Kaygili, I. Ercan, T. Ates, S. Keser, C. Orek, B. Gunduz, T. Seckin, N. Bulut, L. Banares, An experimental and theoretical investigation of the structure of synthesized ZnO powder, Chem. Phys. 513 (2018) 273-279.

[33] T.M.K. Thandavan, S.M.A. Gani, C.S. Wong, R. Md Nor, Evaluation of Williamson–Hall strain and stress distributionin ZnO nanowires prepared using aliphatic alcohol, J. Nondestruct. Eval. 34 (2015) 14.

[34] U. Seetawan, S. Jugsujinda, T. Seetawan, A. Ratchasin, C. Euvananont, C. Junin, C. Thanachayanont, P. Chainaronk, Effect of Calcinations Temperature on Crystallography and Nanoparticless in ZnO Disk, Mater. Sci. Appl. 2 (2011) 1302-1306.

[35] P. Kumar, B.K. Singh, B.N. Pal, P.C. Pandey, Correlation between structural, optical and magnetic properties of Mn-doped ZnO, Applied Physics A 122 (2016) 740.

[36] S.D. Birajdar, R.C. Alange, S.D. More, V.D. Murumkar, K.M. Jadhav, Sol-gel auto combustion synthesis, structural and magnetic properties of Mn doped ZnO nanoparticless, Procedia Manufacturing 20 (2018) 174-180.

[37] Nicole Jones Binata Ray Koodali T. Ranjit Adhar C. Manna, Antibacterial activity of ZnO nanoparticle suspensions on a broad spectrum of microorganisms, 279 (2008) 71–76.

[38] Lingling Zhang, Yunhong Jiang, Yulong Ding, Malcolm Povey, David York, Investigation into the antibacterial behaviour of suspensions of ZnO nanoparticles (ZnO nanofluids), *Journal of Nanoparticle Research,* 9 (2007) 479–489

[39] Laura K. Adams, Delina Y. Lyon, Pedro J.J. Alvarez, Comparative eco-toxicity of nanoscale TiO_2, SiO_2, and ZnO water suspensions, Water research, 40 (2006) 3527-3532.

[40] Kaja Kasemets, Angela Ivask, Henri-Charles, Dubourguier Anne Kahru, Toxicity of nanoparticles of ZnO, CuO and TiO_2 to yeast *Saccharomyces cerevisiae,* Toxicology in Vitro, 23 (2009) 1116-1122.

[41] Mei Li, Lizhong Zhu and Daohui Lin, Toxicity of ZnO Nanoparticles to *Escherichia coli*: Mechanism and the Influence of Medium Components, *Environ. Sci. Technol.*, 45 (5) (2011) 1977–1983

[42] Jun Sawai, [1]Shinobu Shoji, HideoI garashi, Atsushi Hashimoto, Takao Kokugan, Masaru Shimizu, Hiromitsu Kojima, Hydrogen peroxide as an antibacterial factor in zinc oxide powder slurry, Journal of Fermentation and Bioengineering, 86 (1998) 521-522

[43] Anat Lipovsky, Yeshayahu Nitzan, Aharon Gedanken and Rachel Lubart, Antifungal activity of ZnO nanoparticles—the role of ROS mediated cell injury, *Nanotechnology* 22 (2011) 105101

[44] Yuanxun Zhang, James J. Schauer, Martin M. Shafer, Michael P. Hannigan and Steven J. Dutton, Source Apportionment of in Vitro Reactive Oxygen Species Bioassay Activity from Atmospheric Particulate Matter, *Environ. Sci. Technol.*, 42(19) (2008) 7502–7509

[45] Razieh Jalal, Elaheh K. Goharshadi, Maryam Abareshi, Majid Moosavi, Abbas Yousefi, Paul Nancarrow, ZnO nanofluids: Green synthesis, characterization, and antibacterial activity, Materials Chemistry and Physics, 121 (2010) 198-201

[46] Wenhua Song, Jinyang Zhang, Jing Guo, Jinhua Zhang, Feng Ding, Liying Li, Zengtian Sun, Role of the dissolved zinc ion and reactive oxygen species in cytotoxicity of ZnO nanoparticles, Toxicology Letters, 199 (2010) 389-397

[47] Tobias J. Brunner, Peter Wick, Pius Manser, Philipp Spohn, Robert N. Grass, Ludwig K. Limbach, Arie Bruinink, and Wendelin J. Stark, In Vitro Cytotoxicity of Oxide Nanoparticles: Comparison to Asbestos, Silica, and the Effect of Particle Solubility, *Environ. Sci. Technol.*, 40(14) (2006) 4374–4381.

[48] Cory Hanley, Janet Layne, Alex Punnoose, K M Reddy, Isaac Coombs, Andrew Coombs, Kevin Feris and Denise Wingett, Preferential killing of cancer cells and activated human T cells using ZnO nanoparticles, *Nanotechnology* 19 (2008) 295103

[49] Mariappan Premanathan, Krishnamoorthy Karthikeyan, Kadarkaraithangam Jeyasubramanian, Govindasamy Manivannan, Selective toxicity of ZnO nanoparticles toward Gram-positive bacteria and cancer cells by apoptosis through lipid peroxidation Author links open overlay panel, Nanomedicine: Nanotechnology, Biology and Medicine. 7 (2011) 184-192

[50] Philip J. Moos, Kyle Olszewski, Matthew Honeggar, Pamela Cassidy, Sancy Leachman, David Woessner, N. Shane Cutler and John M. Veranth, Responses of human cells to ZnO nanoparticles: a gene transcription study, *Metallomics*, 3 (2011) 1199-1211

[51] T Sugiura, E Kuroda, U Yamashita, Dysfunction of macrophages in metallothionein-knock out mice, Journal of UOEH, 26.2 (2004): 193-205

[52] Ruchi Roy, Sandeep Kumar, Alok K. Verma, Akanksha Sharma, Bhushan P. Chaudhari, Anurag Tripathi, Mukul Das, Premendra D. Dwivedi, Zinc oxide nanoparticles provide an adjuvant effect to ovalbumin via a T_h2 response in Balb/c mice, *International Immunology*, 26 (2014) 159–172.

[53] Verena Wilhelmi, Ute Fischer, Heike Weighardt, Klaus Schulze-Osthoff, Carmen Nickel, Burkhard Stahlmecke, Thomas A. J. Kuhlbusch, Agnes M. Scherbart, Charlotte Esser, Roel P. F. Schins, Catrin Albrecht, Zinc Oxide Nanoparticles Induce Necrosis and Apoptosis in Macrophages in a p47phox- and Nrf2-Independent Manner, *PloS one* 8.6 (2013): e65704

[54] Metka Šimundić,[1] Barbara Drašler,[2] Vid Šuštar,[3] Jernej Zupanc,[2] Roman Štukelj,[4] Darko Makovec,[5] Deniz Erdogmus,[6] Henry Hägerstrand,[7] Damjana Drobne,[2] and Veronika Kralj-Iglič, Effect of engineered TiO_2 and ZnO nanoparticles on erythrocytes, platelet-rich plasma and giant unilamelar phospholipid vesicles, *BMC veterinary research* 9.1 (2013) 7.

 doi:10.20944/preprints201904.0299.v1

[55] Roghayeh Abbasalipourkabir, Salehzadeh Aref, and Abdullah Rasedee, Cytotoxicity effect of solid lipid nanoparticles on human breast cancer cell lines, *Biotechnology* 10.6 (2011) 528-533.

[56] R. Raguvaran, A. Manuja, S. Singh, M. Chopra, B.K. Manuja and U. Dimri, Zinc Oxide Nanoparticles Induced Haemolytic Cytotoxicity in Horse Red Blood Cells. Int J Pharm Sci Res 6(3) (2015) 1166-69.

[57] Roghayeh Abbasalipourkabir, Hemen Moradi, Sadegh Zarei, Soheila Asadi, Aref Salehzadeh, Abolfazl Ghafourikhosroshahi, Motahareh Mortazavi, Nasrin Ziamajidi, Toxicity of zinc oxide nanoparticles on adult male Wistar rats, Food and Chemical Toxicology 84 (2015) 154-160.

[58] K. Kairyte, A. Kadys, Z. Luksiene, Antibacterial and antifungal activity of photoactivated ZnO nanoparticles in suspension, Journal of Photochemistry and Photobiology B: Biology, 128 (2013) 78-84.

Preprints (www.preprints.org) | NOT PEER-REVIEWED | Posted: 26 April 2019 doi:10.20944/preprints201904.0299.v1

Figure Captions:

Fig. 1: A) XRD pattern, **B)** $\beta\cos\theta$ vs. $4\sin\theta$, **C)** $\beta\cos\theta$ vs. $4\sin\theta Y^{-1}$ and **D)** $\beta_{hkl}\cos\theta_{hkl}$ vs. $2^{5/2}\sin\theta_{hkl}\,Y_{hkl}^{-1/2}$ plots of the as-produced ZnO nanostructured.

Fig. 2: SEM images of the as-produced ZnO nanostructured.

Fig. 3: Antimicrobial activity of ZnO nanoparticles against (A) *Candida albicans* and (B) *Staphylococcus aureus* and (C) *E coli*.

Fig. 4: Percent normal splenocytes inhibition after treatment with different concentrations of ZnO nanoparticles.

Fig. 5: Effects of ZnO nanoparticles on normal splenic cells; **A:** normal control splenic cells; **B-F:** normal splenic cells treated with 100, 50, 25, 12.5 and 6 µg/mL ZnO nanoparticles respectively.

Fig. 6: (a) Cytotocity test of ZnO nanoparticles on cow RBCs, where tube ZnO: ZnO nanoparticles, tube N: Negative control (PBS) and tube P: Positive control (1% Triton-X100) and (b) Percent stimulation/inhibition of cancer cell lines after treatment with different concentrations of ZnO nanoparticles.

Preprints (www.preprints.org) | NOT PEER-REVIEWED | Posted: 26 April 2019 doi:10.20944/preprints201904.0299.v1

Table Captions:

Table. 1. Antimicrobial potential of ZnO nanoparticles

Test microorganism	Inhibition Zone (mm)	
	ZnO	Tetracyclin (30)
Staphylococcus aureus	20	17
Bacillus subtilis	12	20
Pseudomonas aeruginosa	15	18
E Coli	22	14
Candida albicans	20	19

Table. 2. Percent of splenic cells growth inhibition after treatment with ZnO nanoparticles.

ZnO nanoparticles (µg/mL)	% of splenic cells growth inhibition of normal rat splenic cells
100	-10.54±0.04
50	-15.63±0.08
25	-17.21±0.14
12.5	-14.11±0.09
6	-15.51±0.06

Preprints (www.preprints.org) | NOT PEER-REVIEWED | Posted: 26 April 2019 doi:10.20944/preprints201904.0299.v1

List of Figures

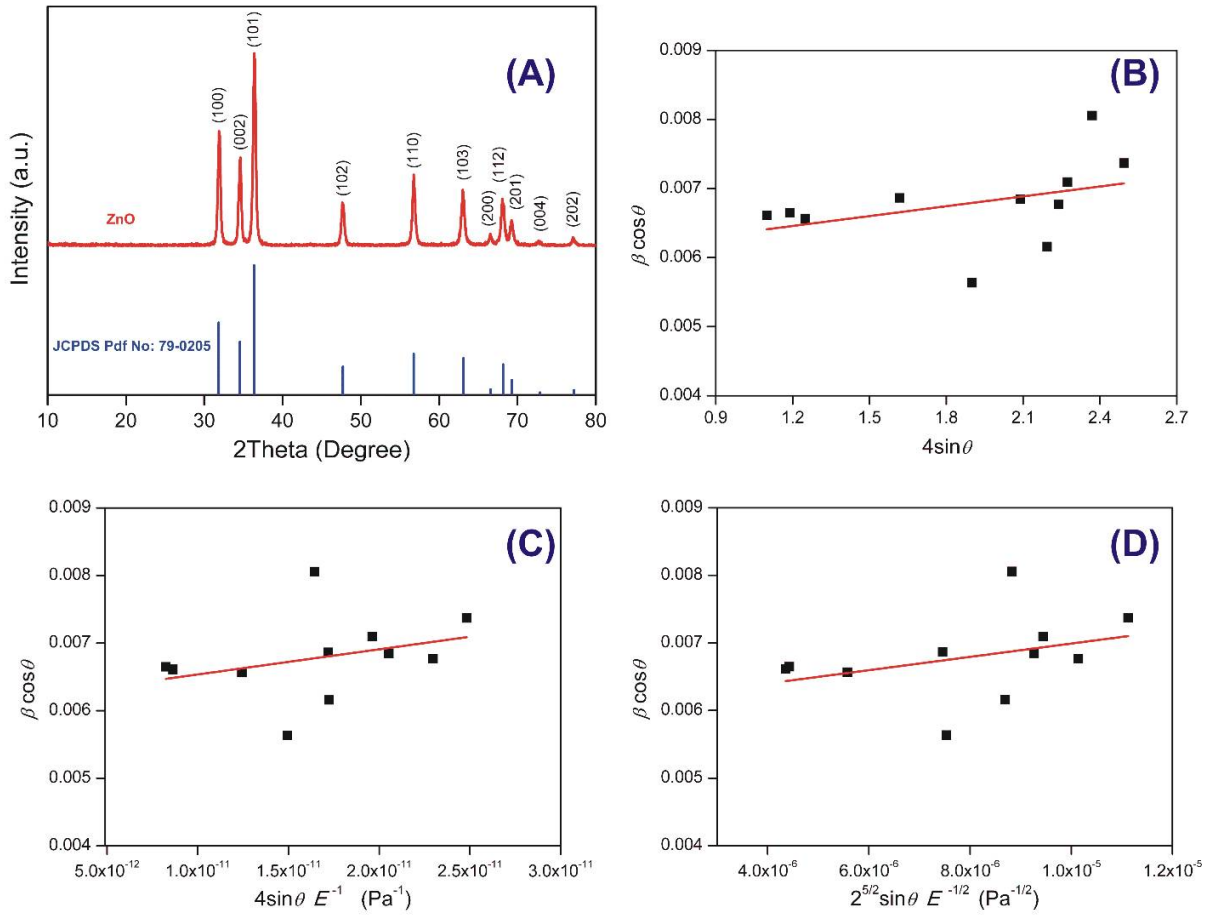

Fig. 1

Preprints (www.preprints.org) | NOT PEER-REVIEWED | Posted: 26 April 2019 doi:10.20944/preprints201904.0299.v1

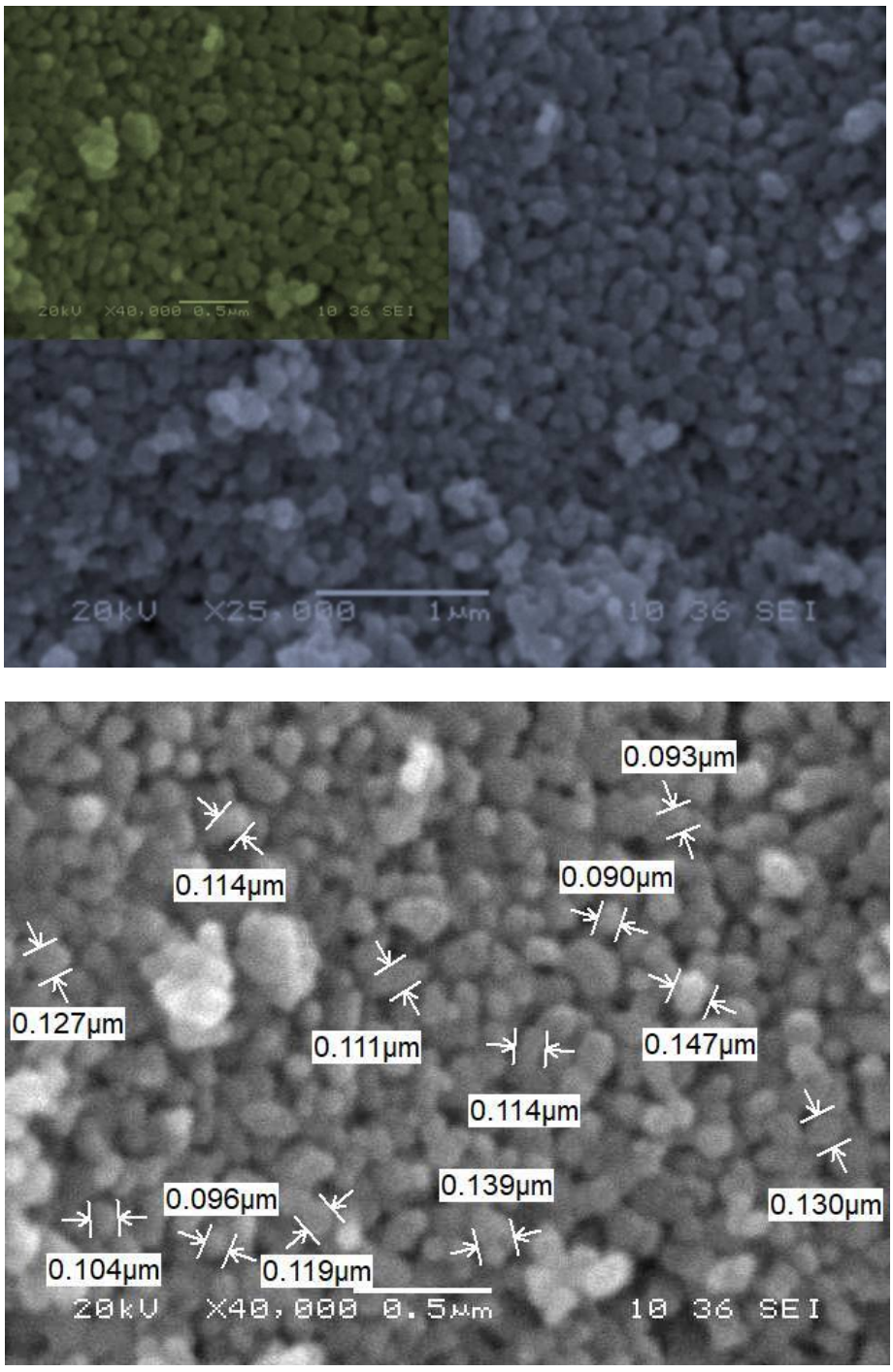

Fig. 2

Preprints (www.preprints.org) | NOT PEER-REVIEWED | Posted: 26 April 2019 doi:10.20944/preprints201904.0299.v1

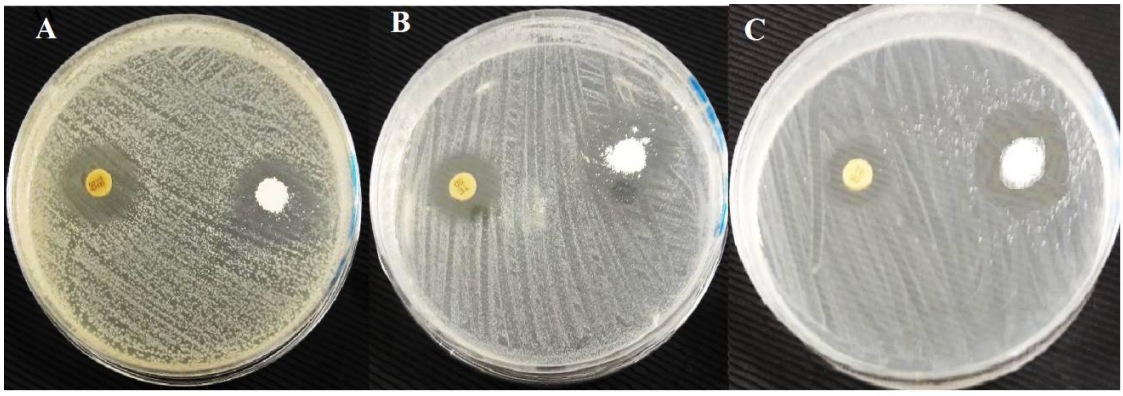

Fig. 3

Preprints (www.preprints.org) | NOT PEER-REVIEWED | Posted: 26 April 2019 doi:10.20944/preprints201904.0299.v1

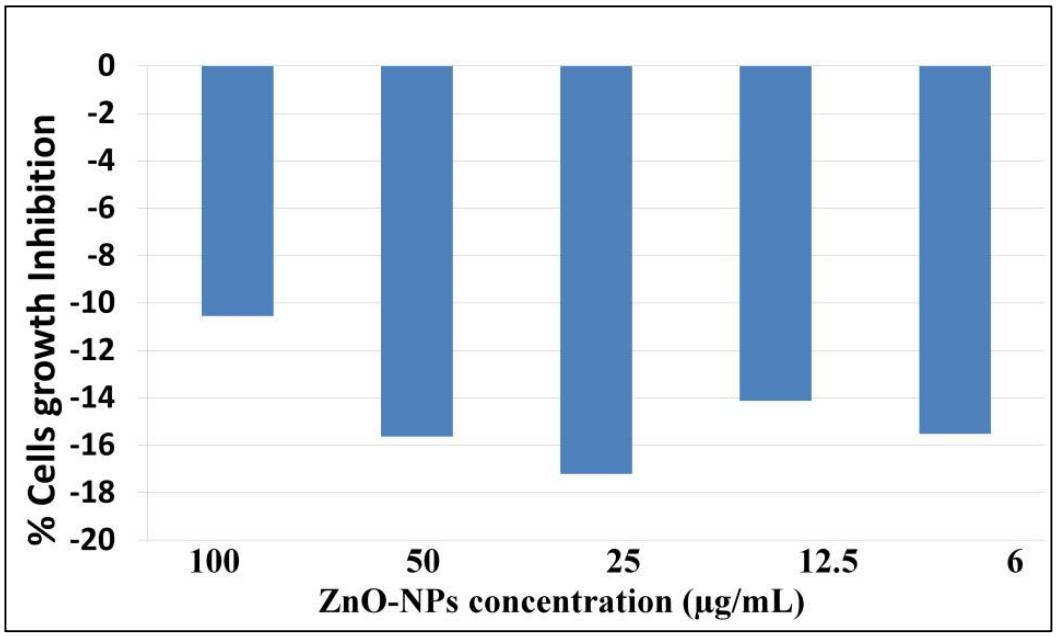

Fig. 4

Preprints (www.preprints.org) | NOT PEER-REVIEWED | Posted: 26 April 2019 doi:10.20944/preprints201904.0299.v1

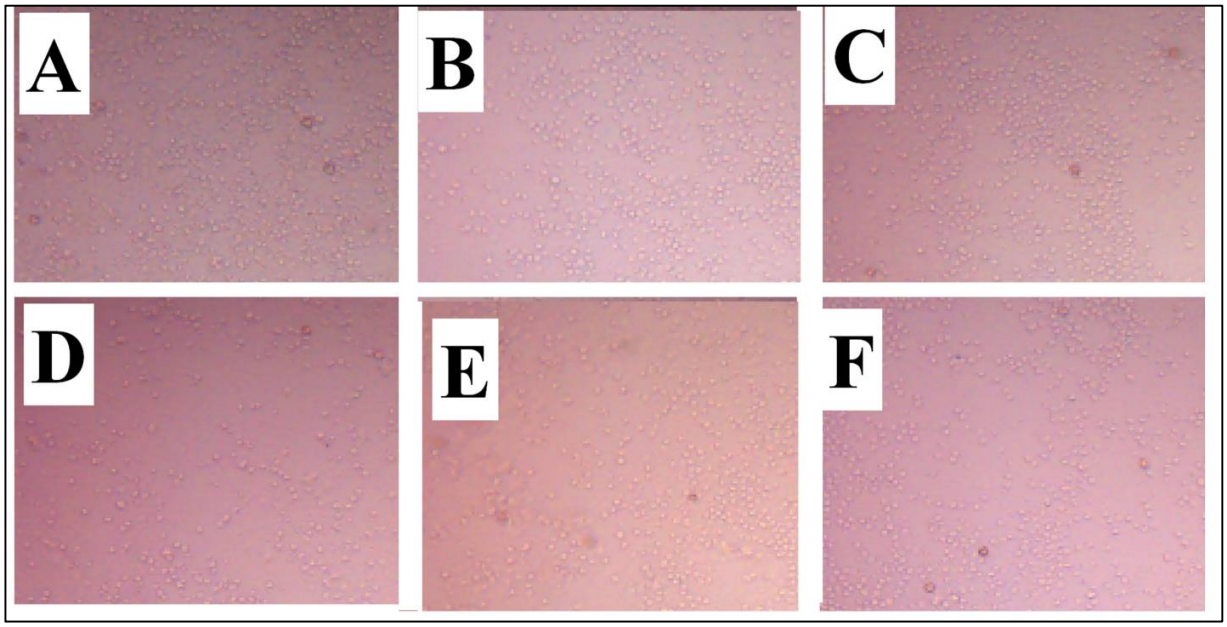

Fig. 5

Preprints (www.preprints.org) | NOT PEER-REVIEWED | Posted: 26 April 2019 doi:10.20944/preprints201904.0299.v1

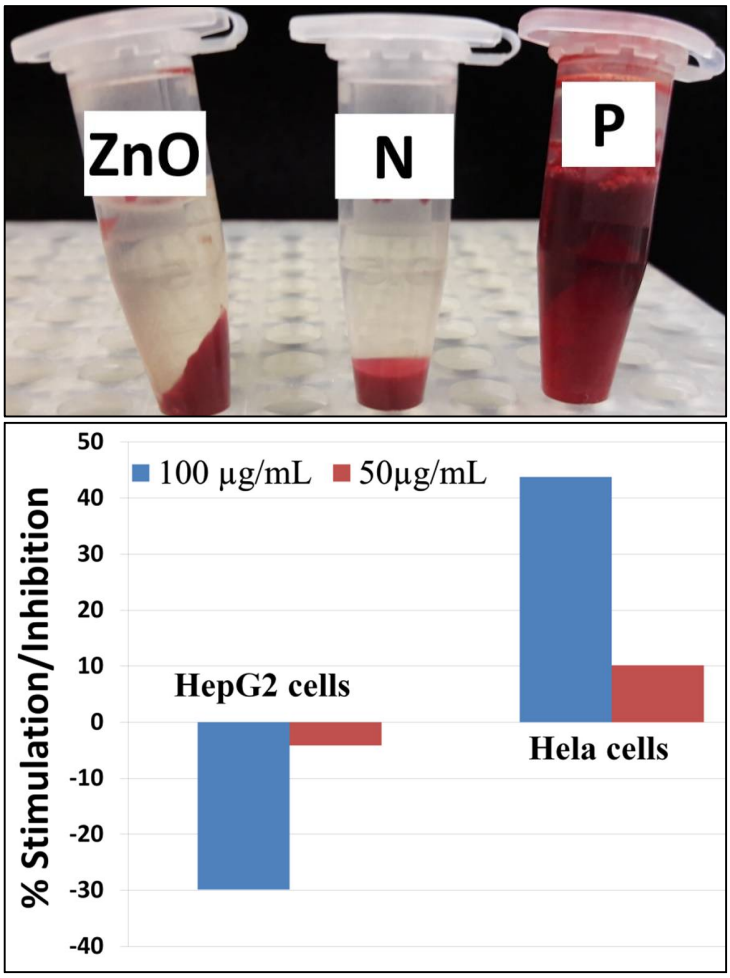

Fig. 6(a) and (b)